

## Magnetoresistance effects in spin-valves comprising Fe<sub>3</sub>Si/N-doped carbon/Fe trilayered films

Satoshi Takeichi<sup>1</sup>, Kazuki Kudo<sup>1</sup>, Kazutoshi Nakashima<sup>1</sup>, Ken-ichiro Sakai<sup>2</sup>, and Tsuyoshi Yoshitake<sup>1</sup>

*<sup>1</sup> Department of Applied Science for Electronics and Materials, Kyushu University, Kasuga, Fukuoka 816-8580, Japan.*

*<sup>2</sup> Department of Control and Information Systems Engineering, National Institute of Technology, Kurume College, Kurume, Fukuoka 830-8555, Japan*

### Abstract

Trilayered spin-valves composed of ferromagnetic Fe<sub>3</sub>Si and Fe layers and nitrogen-doped carbon interlayers were prepared on Si(111) substrates by a mask method, and the injection and transport of polarized carriers were experimentally studied from their magnetic and electrical evaluations. Here, the nitrogen-doped carbon layers were deposited by coaxial arc plasma deposition (CAPD) in the same manner as the deposition of nitrogen-doped ultrananocrystalline diamond (UNCD)/hydrogenated amorphous carbon (a-C:H) composite (UNCD/a-C:H) films comprising a large number of nanodiamond grains embedded in an a-C:H matrix. The shape of a magnetization curve had clear steps, This evidently indicates the formation of antiparallel alignment of the magnetization owing to a difference in the coercive force between the top polycrystalline Fe and bottom epitaxial Fe<sub>3</sub>Si layers. Curiously, the magnetoresistance (MR) curve of the trilayers exhibits negative signal corresponding to the formation of antiparallel magnetization alignments, so-called “inverse MR effects”, which is completely opposite from behavior of the conventional spin-valves that exhibit positive signals.

### 1. Introduction

Electronics and magnetics that utilize electric charge and spin of electrons, respectively, have progressed almost independently until the discovery of giant magnetoresistance (GMR) effects [1,2]. Spintronics is the fusion field of electronics and magnetics, and have attracted considerable attention from physical and practical viewpoints, because both electric charge and spin of electrons are utilized simultaneously. GMR and tunnel magnetoresistance (TMR) [3-5] effects have been the main principles of spintronics devices such as hard disk heads, which use changes in the electrical resistance accompanied by switching between parallel and antiparallel magnetization alignments.

Whereas GMR and TMR films employ nonmagnetic metal and insulator as interlayers, respectively, semiconductor spintronics has also extensively been investigated. Spin-transistors are

representative application candidates [6]. For the application to spin-transistors, spin injection from ferromagnetic metals into semiconductors and spin transport in semiconductors are key. It is expected that materials composed of light elements possess long spin-transport lengths due to weak spin-orbit interactions. In particular, carbon-based materials such as graphene and carbon nanotube (CNT) have received much attention as promising materials of spin-transport [7,8].

In the recent decade, our laboratory has investigated the semiconducting characteristics of ultrananocrystalline diamond (UNCD)/hydrogenated amorphous carbon (a-C:H) composite (UNCD/a-C:H) films comprising a large number of nano-sized diamond grains and an a-C:H matrix, prepared by coaxial arc plasma deposition (CAPD) [9-13]. We have experimentally demonstrated that they can be deposited on foreign solid substrates at low substrate

temperatures by CAPD and p and n-types conduction can be produced by boron and nitrogen doping.

According to previous reports, n-type Si and Ge have longer spin diffusion lengths than those of p-type ones [14-17] and the polarization of MR effects seems not to be dependent on the conduction type. And organic semiconductors exhibits inverse MR effects. Here, note that variable range hopping is predominant in UNCD/a-C:H, similarly to organic semiconductors.

In this work, trilayered spin-valves comprising ferromagnetic Fe<sub>3</sub>Si and Fe electrodes and nitrogen-doped UNCD/a-C:H interlayer were prepared by physical vapor deposition combined with a mask method, and they were studied structurally, magnetically, and electrically.

## 2. Experimental

Fe (100 nm)/nitrogen-doped UNCD (10 nm)/Fe<sub>3</sub>Si (100 nm) trilayered spin-valves were prepared on p-type Si(111) substrates by a mask method. The deposition procedure of the trilayers is shown in Fig. 1(a). Firstly, natural oxide on the p-type Si(111) substrate having specific resistances in the range of 3000-8000  $\Omega\cdot\text{cm}$  was removed with 0.5% hydrofluoric acid and rinsed in deionized water as the pretreatment of substrates. Secondly, the bottom Fe<sub>3</sub>Si layer was deposited on the Si(111) substrate at an Ar pressure of  $1.33 \times 10^{-1}$  Pa and substrate temperature of 300  $^{\circ}\text{C}$ , by facing target direct-current sputtering (FTDCS) using the 1st mask. Subsequently, after the exposure to air for the mask replacement, nitrogen-doped UNCD/a-C:H interlayer was deposited by coaxial arc plasma deposition (CAPD) with the 2nd mask at a substrate temperature of 300  $^{\circ}\text{C}$  under a 53.3 Pa nitrogen and hydrogen mixed gas atmosphere with an inflow ratio between nitrogen and hydrogen gases (IN/H) of 1.5. Finally, after the exposure to air for the mask replacement again, the top Fe layer was deposited with the 3rd mask at an argon pressure of  $1.33 \times 10^{-1}$  Pa and room temperature by FTDCS. The crystallinity of the trilayers was evaluated by

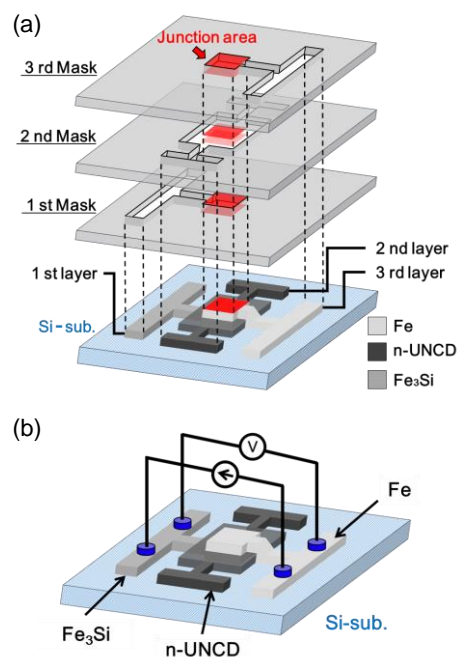


**Figure 1.** Schematic diagram of (a) deposition procedure of Fe/nitrogen-doped UNCD/Fe<sub>3</sub>Si trilayers and (b) electrical circuit for MR curve measurement.

X-ray diffraction (XRD). The magnetization curves of the trilayers were measured at room temperature using a vibrating sample magnetometer (VSM). The electrical circuit for measuring MR effects is schematically shown in Fig. 1(b).

## 3. Result and Discussion

### 3.1. Crystallinity

The 2 $\theta$ - $\theta$  XRD patterns of the trilayers and the Si(111) substrate as a background are shown in Fig. 2(a). Diffraction peaks of Fe<sub>3</sub>Si-222 and Fe-200 are observed. Figure 2(b) shows a pole-figure concerning the Fe<sub>3</sub>Si-422 plane with a rotation axis of Fe<sub>3</sub>Si [222]. It was confirmed that 111-oriented crystallites are also in-plane ordered. Totally considering these results and our previous research [18], the bottom Fe<sub>3</sub>Si layer is epitaxially grown on the Si(111) substrate. Since the Fe layer is deposited on the non-oriented UNCD/a-C:H, it should be polycrystalline.

### 3.2 Magnetical and Electrical Properties

Magnetization and MR curves of the

trilayers, measured at room temperature, are shown in Fig. 3. The magnetization curve has clear two steps that indicate the antiparallel alignment formation of magnetizations owing to the difference in the coercive forces between the top Fe and bottom Fe<sub>3</sub>Si layers.

The MR curve was measured at a bias current of 10 mA. Curiously, corresponding to the switching of layer magnetization alignments, the MR curve exhibits a negative signal. This is because the device-resistance for the antiparallel magnetization alignment is lower than that for the parallel alignment of the FM electrodes.

The origin of this “inverse MR” is unknown at present. In organic semiconductors, it is considered that inverse MR might be induced by an inversion of the spin polarization of the conduction electrons at the oxide- or hybrid-layer formed between ferromagnetic electrode and interlayer as previously reported in spin-valves comprising organic materials such as 8-hydroxy-quinoline aluminium (Alq3), poly(3-hexylthiophene) (P3HT), and C60 [19-21]. For a probable origin, the similar mechanism is supposed.

#### 4. Conclusion

Fe/nitrogen-doped UNCD/Fe<sub>3</sub>Si trilayered spin-valves were prepared by a mask method, and the spin-valve behaviors were magnetically and electrically evaluated. Due to a difference in the coercive force between the top polycrystalline Fe and bottom epitaxial Fe<sub>3</sub>Si layers, the antiparallel alignments of magnetizations were formed. The polarization of the MR curve is opposite to that of general metallic spin-valves, which evidently indicates inverse MR effects occurs in this study. As previously reported in spin-valves comprising organic materials, the inverse MR might be induced by oxide- or hybrid-layer at the interface between FM electrode and interlayer.

#### Acknowledgment

This work was partially financially supported by JSPS KAKENHI Grant Number JP16K14391 and JP15K21594, and

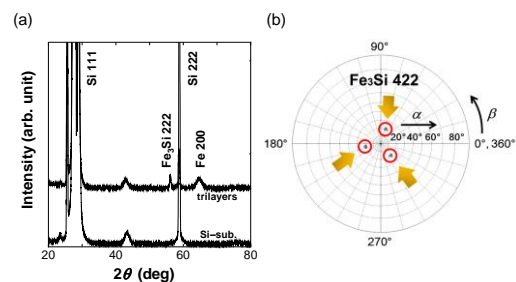


**Figure 2.** (a)  $2\theta$ - $\theta$  XRD patterns of trilayers, and (b) pole figure concerning Fe<sub>3</sub>Si-422 planes.

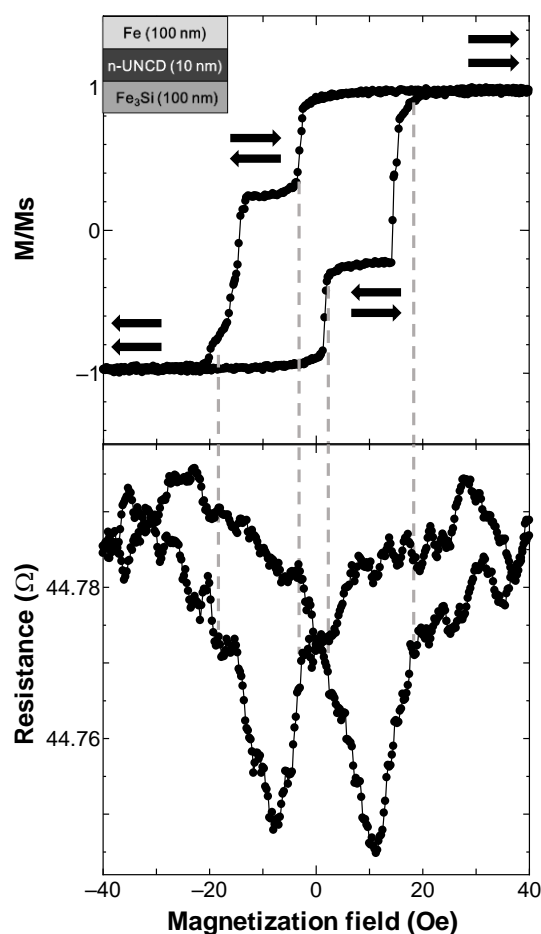


**Figure 3.** Magnetization (upper) and MR (lower) curve of the trilayers, measured at room temperature.

Yoshida Academic Education Promotion Association.

#### Reference

P-14

- [1] G. Binasch, P. Grunberg, F. Saurenbach, and W. Zinn, Phys. Rev. B 39, 4828 (1989).
- [2] M. N. Baibich, J. M. Broto, A. Fert, F. Nguyen Van Dau, F. Petroff, P. Etienne, G. Creuzet, A. Friederich, and J. Chazelas, Phys. Rev. Lett. 61, 247 (1988).
- [3] M. Julliere, Phys. Lett. 54A, 225 (1975).
- [4] S. Maekawa, and U. Gafvert, IEEE Trans. Magn. 18, 707 (1982).
- [5] T. Miyazaki and N. Tezuka, J. Magn. Magn. Mater. 139, L231 (1995).
- [6] S. Sugahara, and M. Tanaka, Appl. Phys. Lett. 84, 2307 (2004)
- [7] M. Shiraishi, Jpn. J. Appl. Phys. 51, 08KA01 (2012).
- [8] K. Tsukagoshi, BW. Alphenaar, and H. Ago, Nature 401, 572 (1999).
- [9] T. Yoshitake, A. Nagano, M. Itakura, N. Kuwano, T. Hara, and K. Nagayama, Jpn. J. Appl. Phys. 46, L936 (2007).
- [10] T. Yoshitake, Y. Nakagawa, A. Nagano, R. Ohtani, H. Setoyama, E. Kobayashi, K. Sumitani, Y. Agawa, and K. Nagayama, Jpn. J. Appl. Phys. 49, 015503 (2010).
- [11] S. Ohmagari, T. Yoshitake, A. Nagano, R. Ohtani, H. Setoyama, E. Kobayashi, T. Hara, and K. Nagayama, Jpn. J. Appl. Phys. 49, 031302 (2010).
- [12] S. Ohmagari and T. Yoshitake, Jpn. J. Appl. Phys. 51, 090123 (2012).
- [13] Y. Katamune, S. Ohmagari, S. Al-Riyami, S. Takagi, M. Shaban, and T. Yoshitake, Jpn. J. Appl. Phys. 52, 065801 (2013).
- [14] S. P. Dash, S. Sharma, R. S. Patel, M. P. de Jong, and R. Jansen, Nature 462, 491 (2009) .
- [15] T. Suzuki, T. Sasaki, T. Oikawa, M. Shiraishi, Y. Suzuki, and K. Noguchi, Appl. Phys. Express 4, 023003 (2011).
- [16] S. Iba, H. Saito, A. Spiesser, S. Watanabe, R. Jansen, S. Yuasa, and K. Ando, Appl. Phys. Express 5, 053004 (2003).
- [17] K. Kasahara, Y. Baba, K. Yamane, Y. Ando, Y. Hoshi, K. Sawano, M. Miyao, and K. Hamaya, J. Appl. Phys. 111, 07C503 (2012).
- [18] K. Takeda, T. Yoshitake, D. Nakagauchi, T. Ogawa, D. Hara, M. Itakura, N. Kuwano, Y. Tomokiyo, T. Kajiwarra, and K. Nagayama, Jpn. J. Appl. Phys. 46, 7846 (2007).
- [19] Z. H. Xiong, Di Wu, Z. Valy Vardeny, and Jing Shi, Nature 427, 821 (2004).
- [20] S. Ding, Y. Tian, Y. Li, W. Mi, H. Dong, X. Zhang, W. hu, and D. Zhu, ACS Appl. Mater. Interfaces 9, 15644 (2017).
- [21] K. Yoshida, I. Hamada, S. Sakata, A. Umeno, M. Tsukada, and K. Hirakawa, Nano Lett. 13, 481 (2013).